Annual Meeting of Korean Society of Coastal and Ocean Engineers
Korea Ocean Research and Development Institute, 11-12 October 1996

Application of time-dependent wave equations to random waves over ripple patch

CHANGHOON LEE[1], KYUNG DOUG SUH[1] and WOO SUN PARK[1]

1 Introduction

In a linear dispersive system, the combined effect of water wave transformations such as refraction, diffraction, shoaling, and reflection can be predicted by the mild-slope equation which was developed by Berkhoff (1972) using the Galerkin-eigenfunction method. In the derivation of the equation, he assumed a mild slope of the bottom $\nabla h/kh \ll 1$ (where ∇ is the horizontal gradient operator, k is the wavenumber, and h is the water depth) and thus neglected second-order bottom effect terms proportional to $O(\nabla h)^2$ and $O(\nabla^2 h)$.

The unsteady time-dependent mild-slope equations (Smith & Sprinks, 1975; Radder & Dingemans, 1985; Kubo et al., 1992; Lee, 1994) were found to properly predict the transformation of narrow-banded random waves with the wave parameters (ω, k, C, C_g, and so on) corresponding to one carrier frequency (Kirby et al., 1992; Kubo et al., 1992). This approach requires less computational time for the solution than the method which uses linear superposition of the solutions of each frequency component.

Recently, by using the Galerkin-eigenfunction method, Massel (1993) and Chamberlain & Porter (1995) developed wave equations intluding the terms of second-order bottom effect for monochromatic waves, and demonstrated the applicability of their equations to rapidly varying bottom topography for which the mild-slope equation could fail to produce adequate approximations. More recently, by using the Green's formula method and the Lagrangian formulation, Suh & Lee (1995) derived two equivalent time-dependent wave equations for the propagation of water waves on rapidly varying bottom topography. Without the terms of second-order bottom effect, each of the derived equations reduces to the time-dependent mild-slope equations developed by Smith & Sprinks and Radder & Dingemans, respectively. A reduced form of the derived equation for a monochromatic wave is the same as the equations developed by Chamberlain & Porter and Massel.

In the present study, we test numerically the time-dependent equations developed by Suh & Lee and Radder & Dingemans for the case of unidirectional random waves normally incident on a finite ripple patch. The numerical solutions are compared against the solution of the Laplace equation by the finite element method (Park et al., 1992), which may be regarded as an exact solution for linear random waves. The test conditions are chosen to be the same as Davies & Heathershaw's (1984) bed with ten ripples for which a marked discrepancy was observed between the results of the mild-slope equation and the equation with terms of second-order bottom effect for the case of a monochromatic wave (Massel, 1993; Chamberlain & Porter, 1995). The schematic diagram of the numerical test is shown in Fig. 1, in which L_p is the wavelength corresponding to the peak frequency f_p of the input frequency spectrum. First, the internal generation of random waves are

[1]Coastal Engineering Division, Korea Ocean Research & Development Institute

presented. Second, numerical simulations of equations are presented. And finally, conclusions are presented.

2 Internal generation of random waves

The TMA shallow-water spectrum is used as the input spectrum:

$$S(f) = \alpha g^2 (2\pi)^{-4} f^{-5} \exp\left[-1.25(f/f_p)^{-4}\right] \gamma^{\exp[-(f/f_p-1)^2/2\sigma^2]} \phi_k(f,h) \tag{1}$$

In the numerical test, the spectral parameter $\alpha = 7.57 \times 10^{-4}$ and the peak enhancement factor $\gamma = 2$ are used, which gives a broad frequency spectrum. The peak frequency f_p is taken to be 0.76 Hz for which $2k_p/K = 1$ (k_p is the wavenumber of water wave corresponding to f_p and $K = 2\pi$ is the wavenumber of the ripple) and thus significant wave reflection from the ripple patch is expected in the vicinity of the peak frequency. The input frequency spectrum at both the lower and upper cutoff frequencies is set to be 10 % of the peak spectrum. In this frequency range, i.e., between 0.59 Hz and 1.63 Hz, 90 % of the total energy of the spectrum is covered and the corresponding significant wave height is 1.58 cm.

A time-series of normally incident random waves is generated internally inside the model boundaries while the waves reflected from the ripple patch are permitted to freely pass across the wavemaker boundary so that unwanted addition of wave energy inside the model domain can be avoided. From the viewpoint of energy transport, Lee (1996) used this technique successfully for the three models developed by Copeland (1985), Radder & Dingemans and Kubo et al. The viewpoint of energy transport suggests the use of the velocity of wave energy as the velocity of the disturbances caused by the incident wave. In the present problem, the velocity of wave energy is

$$C_e = \bar{C}_g \frac{\bar{\omega}}{\omega} \sqrt{1 + \frac{\bar{C}}{\bar{C}_g}\left(\left(\frac{\omega}{\bar{\omega}}\right)^2 - 1\right)} \tag{2}$$

where the overbar is associated with the carrier frequency $\bar{f}$. Waves are generated internally by adding the water surface elevations of incident wave to the computed ones at the wavemaker boundary. The added water surface elevations for random waves are given by

$$\begin{aligned} \eta^* &= 2\tanh(f_p t) \sum_j \frac{C_{ej}\Delta t}{\Delta x} A_j e^{i(k_j x - \omega_j t + \epsilon_j)} \\ &= 2\tanh(f_p t) \frac{\bar{C}_g \Delta t}{\Delta x} \sum_j \tilde{A}_j e^{i(k_j x - \omega_j t + \epsilon_j)} \end{aligned} \tag{3}$$

where

$$\tilde{A}_j = A_j \frac{\bar{\omega}}{\omega_j} \sqrt{1 + \frac{\bar{C}}{\bar{C}_g}\left(\left(\frac{\omega_j}{\bar{\omega}}\right)^2 - 1\right)} \tag{4}$$

A_j is the amplitude of incident wave with the local angular frequency ω_j, ϵ_j is a random phase independent of the frequency, Δx and Δt are the grid spacing and time step, respectively, and the

term $\tanh(f_p t)$ is added for slow start of wave generation. A time-series of free surface elevation of random waves is generated by the inverse Fourier transform of the TMA spectrum with wave amplitudes $\tilde{A}_j$. The time step for the inverse Fourier transform is $\Delta t = T_p/41$ and the total number of time step is 16,384 so that the total time for wave generation is 399.61 T_p. After 399.61 T_p, waves are generated repeatedly with the time-series from the start.

3 Numerical simulation

Suh & Lee's equations are given by

$$\frac{\partial \tilde{\phi}}{\partial t} = -g\eta \tag{5}$$

$$\frac{\partial \eta}{\partial t} = -\nabla \cdot \left(\frac{CC_g}{g} \nabla \tilde{\phi} \right) + \frac{\omega^2 - k^2 CC_g}{g} \tilde{\phi} + \frac{\omega^2}{g} \{ R_1 (\nabla h)^2 + R_2 \nabla^2 h \} \tilde{\phi} \tag{6}$$

where $\tilde{\phi}$ is the velocity potential at mean water level, η is the water surface elevation, C and C_g are the phase speed and group velocity, prespectively, of water waves with carrier angular frequency ω and wavenumber k, and R_1 and R_2 (can be found in Suh & Lee (1995)) are functions of carrier frequency and water depth. Radder & Dingemans' equations may be resulted from Eqs. (5) and (6) if terms with $(\nabla h)^2$ and $\nabla^2 h$ are neglected.

When the frequency spectrum is relatively broad, if a single carrier frequency is used, the solution would become inaccurate for the wave components far from the carrier frequency. In order to obtain better accuracy, the entire frequency range could be divided into several bands and at each band a solution could be obtained with a representative carrier frequency. In the present study, three cases with different number of frequency bands, one, two, and three are examined. The frequency bands are subdivided so that each band contains the same energy, and the carrier frequencies are selected as the weight-averaged frequencies. If the frequency bands are infinitely large, the local frequency would be equal to the carrier frequency and the solution would give the power spectrum of transmitted waves as shown in Fig. 2.

A sponge layer is placed at both upwave and downwave boundaries to minimize wave reflection from the boundaries by dissipating wave energy inside the sponge layers. The thickness of the sponge layer, S, is taken as 2.5 times the longest wavelength of the waves to be modelled. Eq. (5) is modified to

$$\tilde{\phi}_t = -g\eta - \omega_{max} D \tilde{\phi} \tag{7}$$

where ω_{max} is the maximum angular frequency of the waves to be modelled and the damping coefficient D increases exponentially from zero at the starting point of the sponge layer to one at the end.

Eqs. (6) and (7) are discretized by a fourth-order Adams-Moulton predictor-corrector method in time and by a three-point symmetric formula in space. All the values at the initial stage are set to be zero. At both upwave and downwave boundaries, perfect reflection is assumed. However, the

effect of the reflection from these boundaries is negligibly small in the region of interest because the sponge layer significantly reduces the incoming waves. The grid spacing Δx is chosen so that the local wave length is greater than $10\Delta x$ and a spatial resolution is guaranteed. The time step $\Delta t = T_p/328$ is chosen so that the Courant number $C_r = C_e\Delta t/\Delta x$ is less than 0.1 and a stable solution is guaranteed. Since the time step of $T_p/41$ is used for wave generation, a linear interpolation is made to obtain the surface elevations of $\Delta t = T_p/328$ at the wavemaker.

Surface elevations are recorded at a point downwave from the ripple patch to calculate the spectrum of the waves transmitting over the ripple patch. After generating waves, recording is made from $50T_p$ to $449.61T_p$ with the sampling interval of $T_p/53$ so that the total number of sample is 16,384. The 16,384 data points were processed in four segments of 4,096 points per segment. These segments overlap by 50% for smoother and statistically more significant spectral estimates. The raw spectra are then ensemble-averaged. Further smoothing is made by band-averaging over five neighboring frequency bands.

Fig. 2 shows the comparison of the power spectra of transmitted waves over the ripple patch for the FEM solution, Suh & Lee's equation, and mild-slope equation, which are obtained from the input spectrum and reflection coefficients at each frequency using the condition of wave energy conservation $K_r^2 + K_t^2 = 1$ (K_r is the reflection coefficient and K_t is the transmission coefficient). For both the FEM solution and Suh & Lee's equation, the power spectrum of the transmitted waves shows significant reduction around the peak frequency due to the resonant Bragg reflection of incident waves. However, the mild-slope equation yields only a slight reduction around the peak frequency. The significant wave heights of transmitted waves are 1.51 cm (4 % reduction from the incident wave) for both the FEM solution and Suh & Lee's equation, and 1.57 cm (1 %) for the mild-slope equation.

Figs. 3 - 4 show the comparsion of power spectra of the transmitted waves with different number of frequency bands yielded by the Suh & Lee's and Radder & Dingemans' equations, respectively. As the band number increases, the power spectrum becomes closer to that of infinitely large frequency bands, which proves the better accuracy of the solution with narrower frequency bands. The significant wave heights yielded by the Suh & Lee's equation are 1.57 cm (4 % error compared to the solution, H_s = 1.51 cm, with infinitely large frequency bands), 1.52 cm (1 % error), and 1.51 cm (0 % error) for the case of one, two, and three frequency bands, respectively. The significant wave heights yielded by the Radder & Dingemans' equation are 1.55 cm (-1 % error compared to the solution, H_s = 1.57 cm, with infintely large frequency bands), 1.57 cm (0 % error), and 1.57 cm (0 % error) for the case of one, two, and three frequency bands, respectively.

4 Conclusions

In order to see how the wave equations with and without terms of second-order bottom effect yield solutions for random waves on rapidly varying topography, the unsteady time-dependent wave equations developed by Suh & Lee (1995) and Radder & Dingemans (1985) have been tested for the Bragg reflection of random waves normally incident on a finite ripple patch. The solutions were compared to the solution of the Laplace equation by a fininte element method. For Suh & Lee's equation, the feature of the Bragg reflection of random waves was found to be very similar to the solution by the finite element method, that is, the wave components whose frequency is nearly or exactly resonant with the bottom experience fairly significant reflection by the ripple patch, while

the reflection is very small for the wave components whose frequency is far out of the resonant frequency. However, for Radder & Dingemans' equation, the resonant Bragg reflection around the peak frquency was found to be meagre. As the number of frequency bands increased and so the bandwidth became narrower, the numerical solution got closer to the solution with infinitely large frequency bands, which proves that the unsteady time-dependent wave equations yield better solutions with narrower frequency bands.

5 References

Berkhoff, J. C. W. (1972). "Computation of combined refraction-diffraction." *Proc. 13th Intl. Conf. Coastal Eng.*, ASCE, Vancouver, 471-490.

Chamberlain, P. G. and Porter, D. (1995). "The modified mild-slope equation." *J. Fluid Mech.*, 291, 393-407.

Copeland, G. J. M. (1985). "A practical alternative to the mild-slope wave equation." *Coastal Eng.*, 9, 125-149.

Davies, A. G. and Heathershaw, A. D. (1984). "Surface-wave propagation over sinusoidally varying topography." *J. Fluid Mech.*, 144, 419-443.

Kirby, J. T., Lee, C., and Rasmussen, C. (1992). "Time-dependent solutions of the mild-slope wave equation." *Proc. 23rd Intl. Conf. Coastal Eng.*, ASCE, Venice, 391-404.

Kubo, Y., Kotake, Y., Isobe, M., and Watanabe, A. (1992). "Time-dependent mild slope equation for random waves." *Proc. 23rd Intl. Conf. Coastal Eng.*, ASCE, Venice, 419-431.

Lee, C. (1994). *A Study of Time-Dependent Mild-Slope Equations*, Ph.D. Dissertation, Univ. of Delaware.

Lee, C. (1996). "Internal generation of waves for time-dependent mild-slope equations, *Coastal Eng.* (submitted).

Massel, S. R. (1993). "Extended refraction-diffraction equation for surface waves." *Coastal Eng.*, 19, 97-126.

Park, W.-S., Lee, D.-S., Oh, Y.-M., and Jeong, W.-M. (1992). "Infinite elements for analysis of wave diffraction and radiation problems in the vertical plane." *J. Korean Society of Coastal and Ocean Engineers*, 3, 235-243 (in Korean).

Radder, A. C. and Dingemans, M. W. (1985). "Canonical equations for almost periodic, weakly nonlinear gravity waves." *Wave Motion*, 7, 473-485.

Smith, R. and Sprinks, T. (1975). "Scattering of surface waves by a conical island." *J. Fluid Mech.*, 72, 373-384.

Suh, K. D. and Lee, C. (1995). "Time-dependent wave equations on bottom with substantial depth variation." *Proc. Annual Meeting of Korean Society of Coastal and Ocean Engineers*, Sung Kyun Kwan Univ., 75-80.

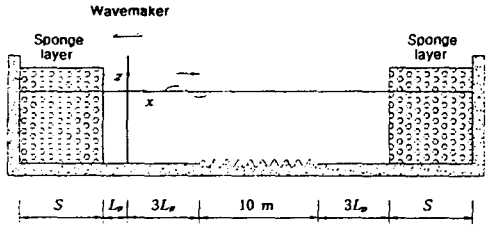

Fig. 1: Schematic diagram for numerical test.

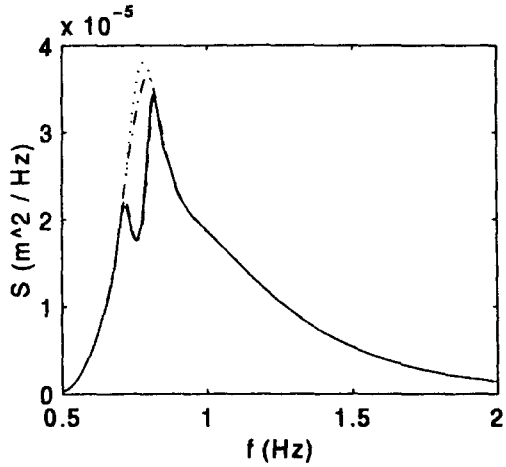

Fig. 2: Power specrtra of incident and transmitted waves ; - - - - = incident wave, — — = transmitted wave for FEM solution, – – – = transmitted wave for Suh & Lee's eq., –·–·– = transmitted wave for Radder & Dingemans' eq.

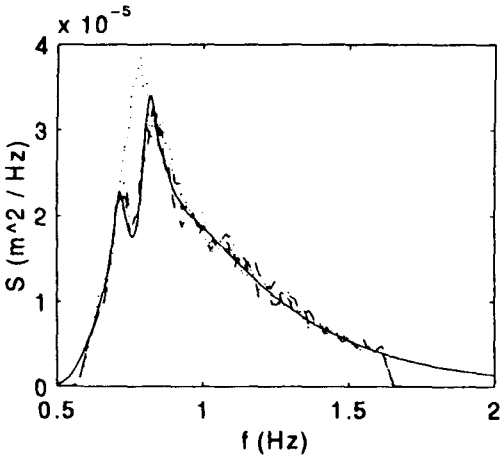

Fig. 3: Power spectra of transmitted waves with different number of frequency bands yielded by Suh & Lee's eq. ; - - - - = one band; –·–·– = two bands, – – – = three bands, —— = infinitely large bands.

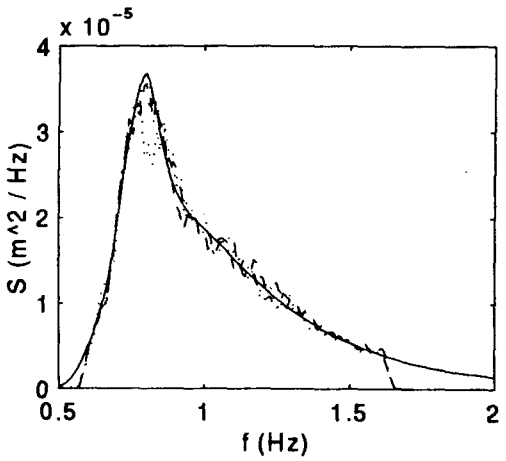

Fig. 4: Power spectra of transmitted waves with different number of frequency bands yielded by Radder & Dingemans' eq. ; - - - - = one band; –·–·– = two bands, – – – = three bands, —— = infinitely large bands.